AD-A139 786 ANALYSIS OF AIRBORNE ELECTROMAGNETIC SYSTEMS FOR MAPPING THICKNESS OF SEA ICE(U) NAVAL OCEAN RESEARCH AND DEVELOPMENT ACTIVITY NSTL STATION MS 1/1

UNCLASSIFIED A BECKER ET AL. NOV 83 NORDA-TN-261 F/G 8/12 NL

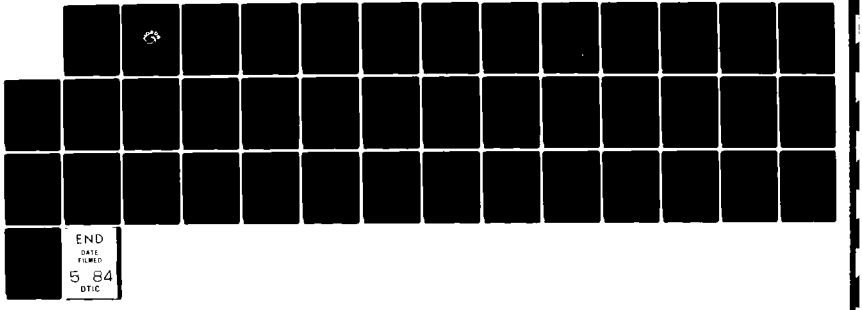

END
DATE FILMED
5 84
DTIC

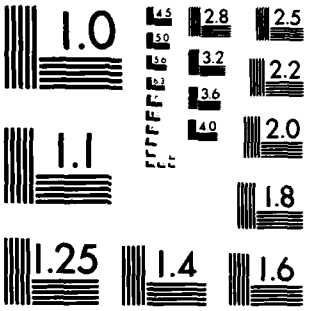

NORDA Technical Note 261

Naval Ocean Research and
Development Activity
NSTL, Mississippi 39529

Analysis of Airborne Electromagnetic Systems for Mapping Thickness of Sea Ice

A. Becker
H. Morrison

University of California
Berkeley, California 94720

K. Smits

Ocean Science Directorate
Mapping Charting and Geodesy Division

November 1983

ABSTRACT

NORDA Code 372 is at present engaged in research projects for extending Airborne Electromagnetic (AEM) technology from geophysical prospecting applications to Navy requirements such as airborne shallow water bathymetry, airborne ice thickness determination, and conductivity profiling. This report is part of our research program addressing AEM ice thickness determination and will demonstrate that the Navy requirements for rapid airborne methods for mapping ice thickness, in real time, can be accomplished with AEM techniques. At present there are not reliable airborne techniques for measuring directly sea ice thickness, although impulse radar has yielded promising results by implying sea ice thickness from ice roughness measurements.

The preparation of this technical note was part of the work performed for extending Airborne Electromagnetic (AEM) technology from geophysical prospecting to ice thickness measurements under Program Element 62759N. Sponsorship was provided by Mr. Barry Dillon of NAVAIRSYMCOM/Code 340. The AEM program is managed by Mr. Kuno Smits, NORDA Code 372. The work was performed during the period May-August 1983.

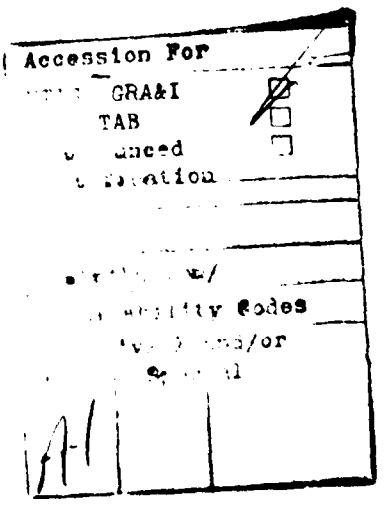

1 Summary

This report examines the feasibility of using an airborne electromagnetic induction apparatus for the mapping of sea ice thickness. After a review of available commercial systems and the electrical properties of sea ice it can be concluded that this novel use of airborne electromagnetics is indeed very feasible.

In order to take full advantage of this technique we suggest a design for an airborne system that is optimal for the designated task of sea ice mapping. Before going on to its construction however, we strongly recommend that the theoretical ideas presented in this report be field tested to ensure that all sources of error have been accounted for. The required field test can be done with conventional contractor apparatus.

2. Introduction

Airborne electromagnetic induction systems have now seen nearly thirty years of commercial service. Traditionally, this type of geophysical exploration equipment is optimized for the detection of discrete, highly conductive mineral deposits which occasionally prove to be of economic value. More recently, airborne electromagnetic apparatus has been used for geological mapping and the related indirect indication of economic minerals. Because of the fair degree of success that was reported in interpreting

airborne electromagnetic data in terms of an underlying geological section (e.g. DeMoully and Becker 1982), it was only natural that one would enquire as to the possible oceanographic applications of this type of apparatus. In this context, Morrison and Becker (1982) reviewed the possible use of airborne electromagnetics for coastal bathymetry. Similarly, this report examines the feasibility of another possible oceanographic application of airborne electromagnetic namely, the mapping of sea ice thickness.

3 Airborne Electromagnetic (AEM) Instrumentation

3.1 Principles

All airborne electromagnetic (AEM) systems basically consist of a primary field source (transmitter) which produces a time dependent magnetic field and a detector (receiver) which senses the secondary magnetic field produced by the eddy currents in the earth. The first system of this kind was developed some twenty-five years ago in Canada for the purpose of mineral exploration. Since then a large variety of AEM systems have been put into production. A majority of these have now been abandoned for one reason or another. In particular at the time of the last review of the state of the art in this field (Becker 1979), nearly a dozen different systems were available for survey work. At present, this abundance has basically been reduced to two AEM systems, (c.f. Figure 1) namely the towed-bird, time-domain INPUT system which is used for about 70% worldwide

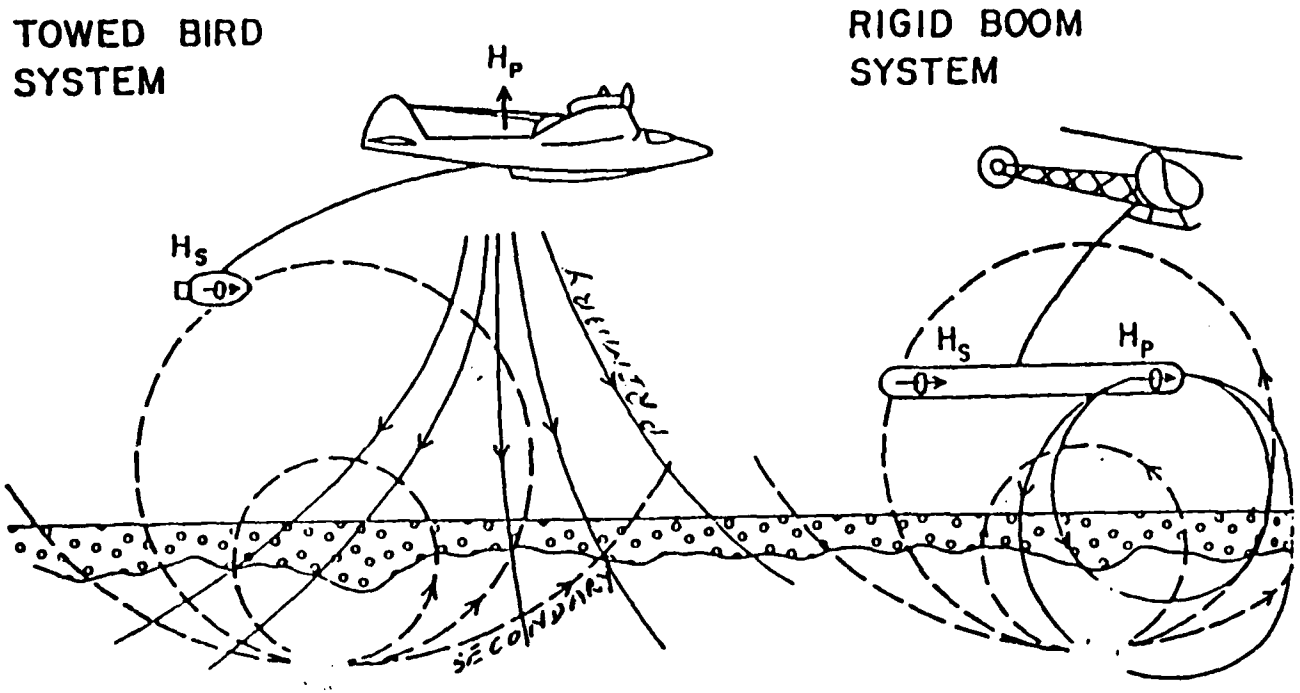

FIGURE 1

AEM SYSTEM CONFIGURATIONS

survey work and the rigid-boom helicopter towed frequency domain system which accounts for about 25% of the work. The remaining 5% of the work is done with special purpose and experimental systems.

The two available systems differ widely in scale but overlap in the frequency range covered. Figures 2 and 3 graphically illustrate this point. While the INPUT system operates in the time-domain transmitting an interrupted, high-power, half sine pulse, it can be shown by Fourier analysis that it covers all the odd harmonics of its fundamental frequency (144 Hz) up to about 5 kHz. The helicopter system operates in the frequency domain and covers a limited frequency range. Normally, both systems detect the horizontal component of the secondary field. On demand, however, either system may be modified to measure the vertical component of the secondary field or, if need be, both components.

3.2 Time Domain Equipment

The INPUT (Induced Pulse Transient) system was invented some twenty years ago by A. R. Barringer (Barringer 1962) and has been modified a number of times since it was first rendered operational. It uses a high power 1 millisecond pulse to induce eddy currents in the ground. The secondary magnetic field related to the decay of these eddy currents is then detected while the primary field is off. The detection of the weak secondary fields during the absence of any

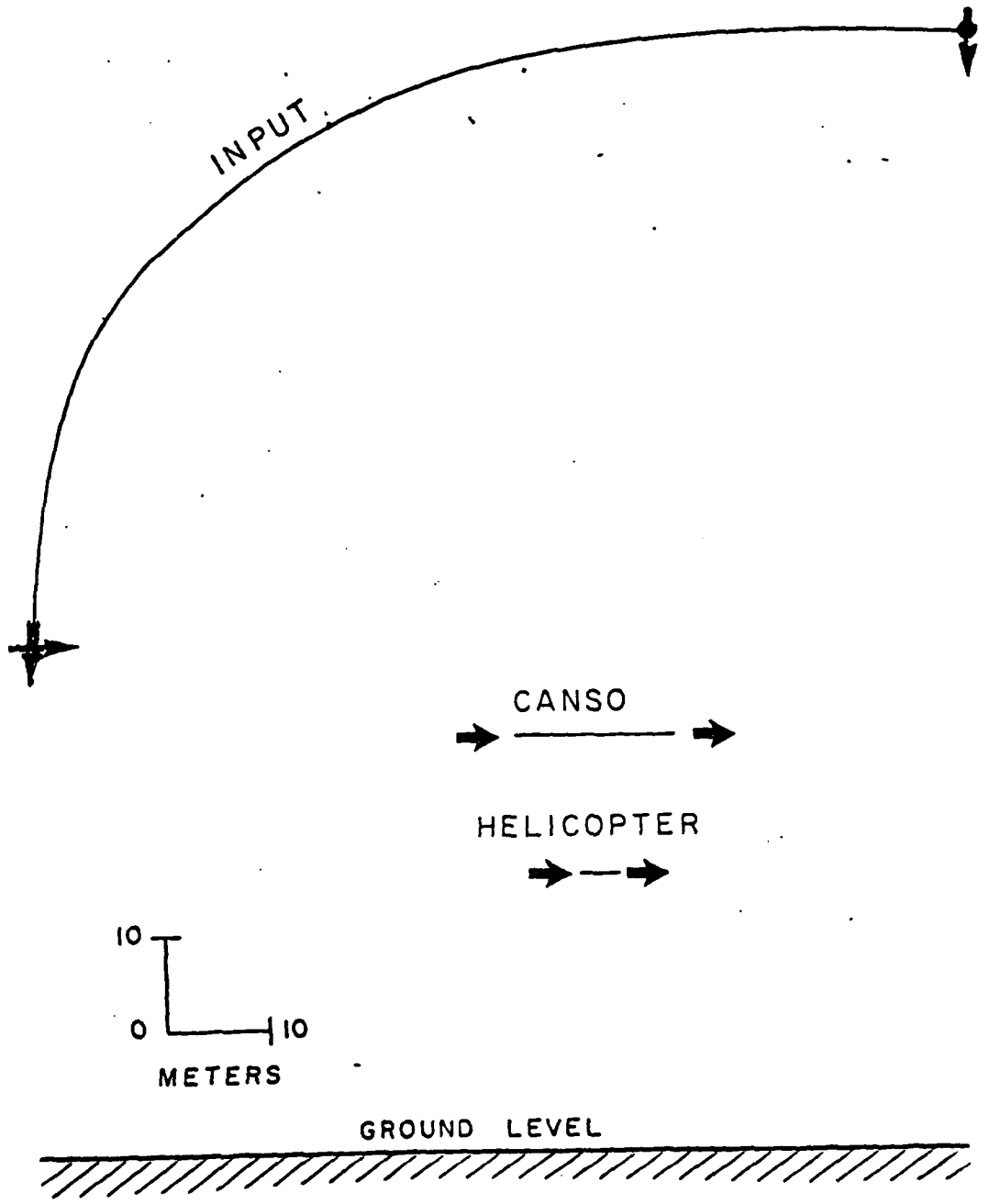

FIGURE 2. AEM SYSTEM GEOMETRY

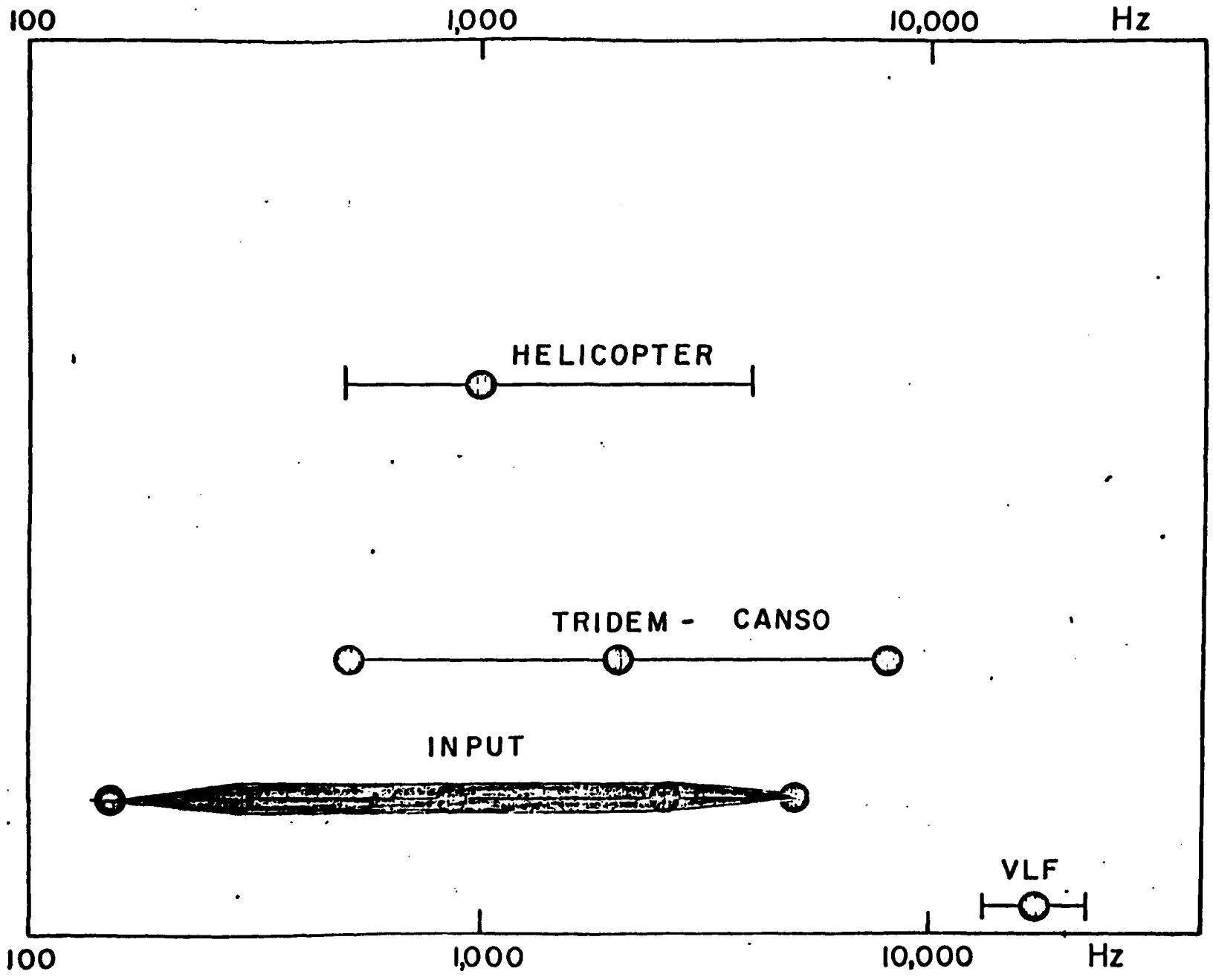

FIGURE 3 AEM SYSTEM FREQUENCIES

strong primary fields avoids electrical dynamic range problems and allows the use of a towed-bird receiver. Similarly, because the primary field is off while the secondary field is detected, one can tolerate a fair amount of motion of the detector with respect to the aircraft without any serious degeneration of the signal quality. The transient signal is sampled at a number of times after the cessation of the primary field. Each sample is then fed to a detector channel (of which there usually are six) and averaged over about 150 repetitions of the primary pulse. The average value of each channel is then displayed on an analog record as a function of distance along the flight path. A detailed analysis of this system was made by Becker (1967) while Palacky (1972) provides a description of the most recent version of this apparatus.

3.3 Frequency Domain Equipment

Figure 4 is a schematic diagram of a typical helicopter frequency domain system. Note the rigidly mounted transmitter and receiver which allows the cancellation of the primary field at the receiver and thus permits the precise measurement of the in-phase and quadrature components of the secondary field in units of parts per million (ppm) of the primary field. A recent description of this type of system, mounted on a helicopter-towed 9m boom, is given by Fraser (1979). Usually as shown in the sketch, the helicopter also tows a magnetometer. Flight path recovery is

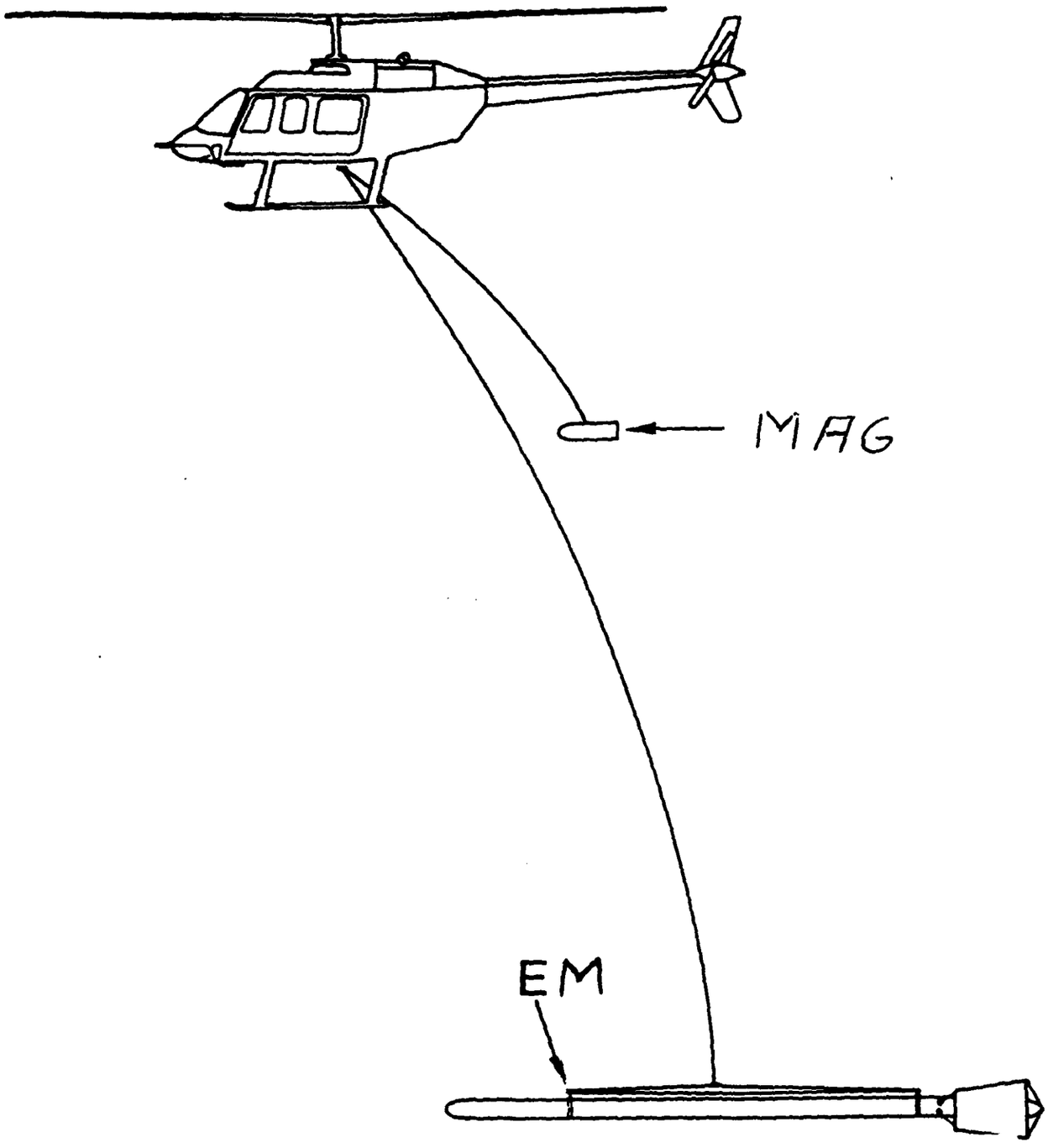

FIGURE 4 CONVENTIONAL HELICOPTER EM

done with the aid of an on board film strip camera. The helicopter also carries a radar altimeter so that its elevation with respect to the ground is known precisely. It should be noted however that the position of the EM boom with respect to the helicopter is only known approximately.

The electrical circuit used in a rigidly coupled frequency electromagnetic system is shown in Figure 5. An electrical link exists between the transmitting and receiving elements. It is used to cancel the voltage induced in the receiver by the primary field and to provide a phase reference for the detection and measurement of the secondary field.

The technical specifications for rigidly coupled frequency domain airborne systems are given in Table 1. The helicopter-towed apparatus is available on a regular commerical basis. The fixed wing equipment operated by Kenting Geophysics in Calgary Canada is available on demand. This system is described by Pitcher et al (1980). With the exception of the larger coil separation and of necessity, larger flight altitude, the fixed wing system operates in an identical fashion to the helicopter-towed boom.

4 Review of Previous Work

4.1 Electromagnetic Measurements

There are no known attempts at measuring the thickness of sea ice with an airborne electromagnetic induction

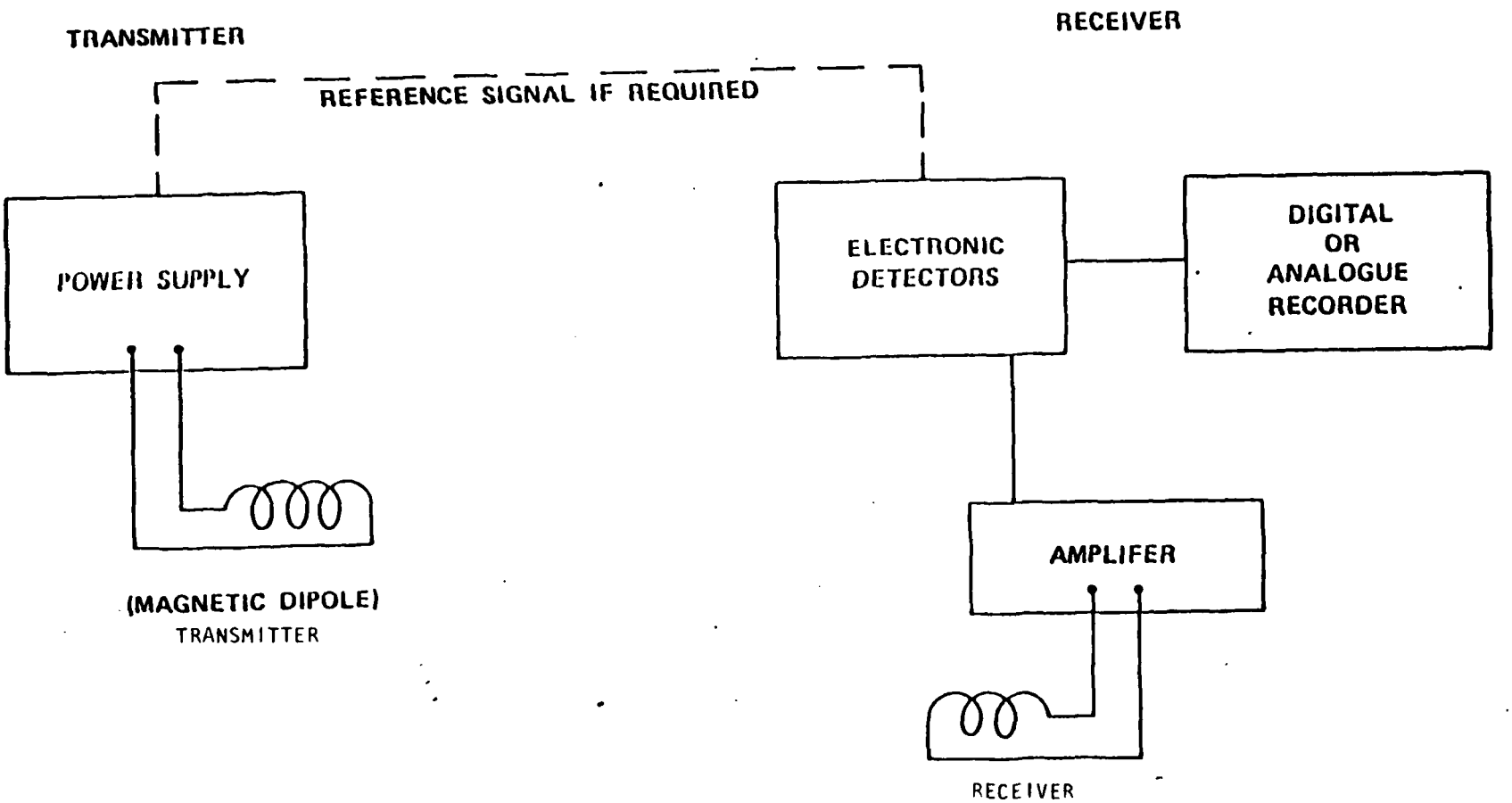

FIGURE 5

FREQUENCY DOMAIN SCHEMATIC

TABLE 1

COMMERICAL RIGID - BOOM
AIRBORNE EM SYSTEMS

	COMMERCIAL NAME	COIL SEPARATION	CONFIGURATION	FREQ. Hz
HELICOPTER	DIGHEM II	9M	COAXIAL	3600
			COPLANAR	900
	AERODAT	6M	COAXIAL	945
			COPLANAR	4022
			COAXIAL	5465
	REXHEM	8M	COAXIAL	736
			COPLANAR	1800
			COAXIAL	4150
FIXED WING	TRIDEM	25M	COAXIAL	500
	PBY			2000
	(KENTING/SCINTREX)			8000

apparatus. Keller and Frischknecht however provide an account of such a measurement that was made with ground electromagnetic equipment over thick ice in the Arctic. The work was done in June 1959 (Keller and Frischknecht 1966, pp. 345-346) in an area where the ice was about 5 meters thick and the water had a conductivity of about 3.2 s/M. Eighty soundings were made using a coil separation of the order of 100m and a primary field excitation in the audio frequency range. Because the system was not absolutely calibrated readings were taken at a number of frequencies and a curve matching procedure was used to interpret the results. On the average, the electromagnetic determinations of ice thickness appeared to be accurate to about 10%.

More recently Sinha (1976) conducted a limited field study to evaluate the usefulness of a light weight, small, high frequency portable electromagnetic prospecting system for the determination of sea ice thickness. Two different pieces of commercial equipment were used. Both had a coil separation of about one meter but differed in frequency of operation with one system running at 15 kHz while the second one operated at 8 kHz. Once again difficulties were encountered with the calibration of the equipment and only the vertical gradient of the system response could be properly measured. The ice thickness was then determined from this quantity. Under favourable circumstances accuracies of a few centimeters in young, thin, (25-75m) ice could be attained.

4.2 Sea Ice Properties

Perhaps the most reliable set of data on the electrical properties of sea ice was obtained by McNeil and Hoekstra (1975) when they attempted to measure the thickness of sea ice by measuring the wave-tilt of VLF transmissions. Although this work, done in the vicinity of the Naval Arctic Research Laboratory at Point Barrow, Alaska in May 1971 failed to prove the usefulness of the wave-tilt method for the desired purpose, it did result in a fairly complete set of data on the electrical properties of sea-ice. Figure 6 shows a summary of their measurements. The data clearly shows that young first year ice retains much of its salinity and is fairly conductive while multi-year ice is gradational in resistivity. As expected, multi-year ice shows a continuous progression from a high resistivity of about 10 K-Ohm-m at surface, to less than 30 Ohm-m at the sea water surface.

Based on the McNeill-Hoekstra data, we have constructed some sea ice models which were then used to evaluate the feasibility of doing a test of airborne electromagnetic sea ice thickness determination. Other sea ice models were then used to determine the response of an optimal system especially designed for sea ice thickness mapping. A summary of the models used in this report is given in Table 2.

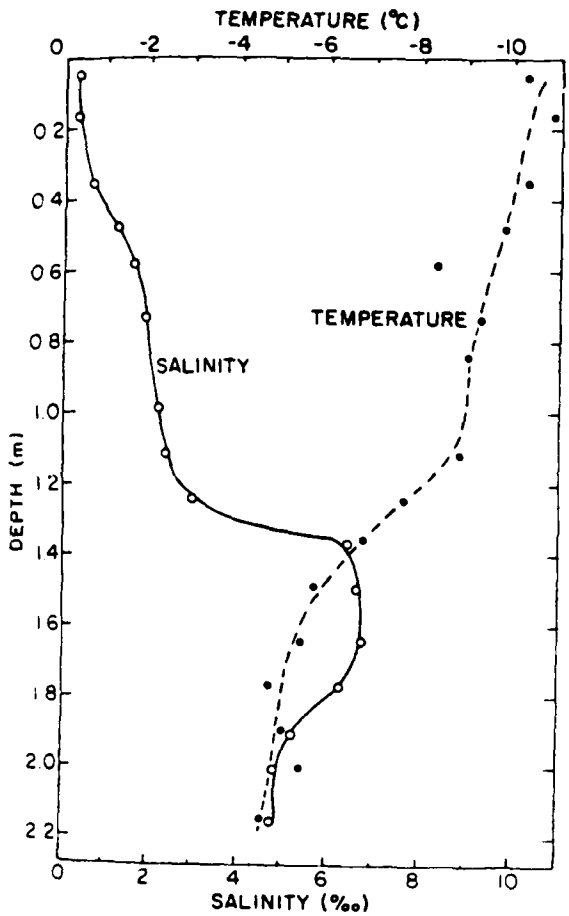

Temperature and salinity distribution for typical multiyear sea ice as a function of depth below the ice surface.

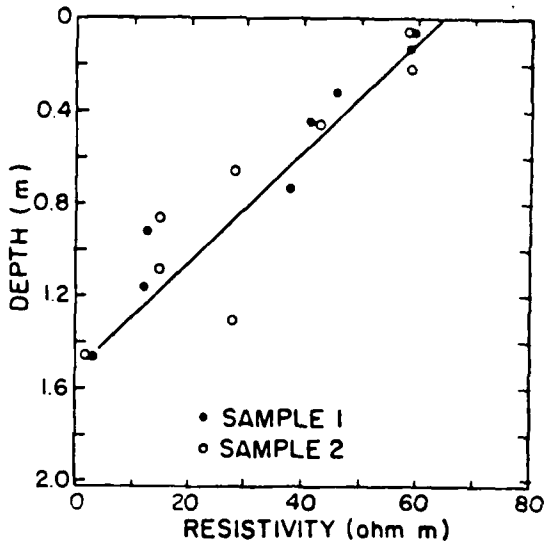

Vertical resistivity profile of typical first-year sea ice measured at 18.6 kHz.

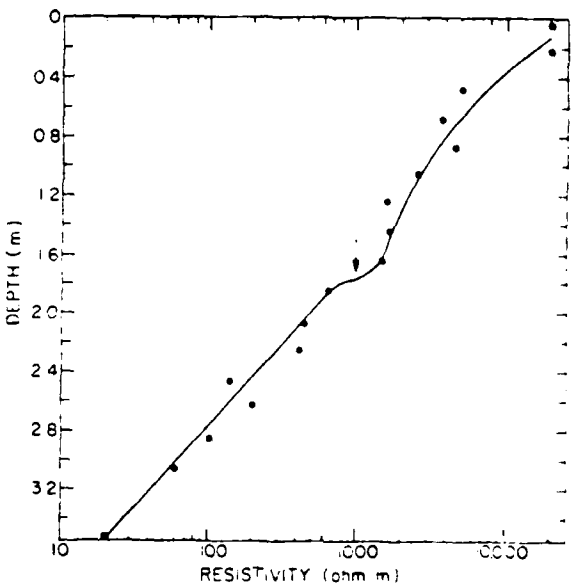

Vertical resistivity profile of typical multiyear sea ice measured at 18.6 kHz.

FIGURE 6 PHYSICAL PROPERTIES OF SEA ICE.
(After McNeill and Hoekstra, 1975)

TABLE 2

TRANSITIONAL MODELS

MULTIYEAR ICE - THICKNESS T

MODEL 1	0 - 0.2T	ρ = 5000Ω-M
	0.2T - 0.4T	ρ = 1500Ω-M
	0.4T - 0.6T	ρ = 200Ω-M
	0.6T - 0.8T	ρ = 30Ω-M
	0.8T - T	ρ = 5Ω-M
MODEL 2	0 - 0.25T	ρ = 100Ω-M
	0.25T - 0.40T	ρ = 70Ω-M
	0.40T - 0.55T	ρ = 45Ω-M
	0.55T - 0.70T	ρ = 15Ω-M
	0.70T - 0.85T	ρ = 5Ω-M
	0.85T - T	ρ = 1Ω-M
MODEL 3	0 - 0.5T	ρ = 100Ω-M
	0.5T - T	ρ = 10Ω-M
MODEL 4	0 - 0.5T	ρ = 100Ω-M
	0.5T - 0.75T	ρ = 50Ω-M
	0.75T - T	ρ = 20Ω-M
MODEL 5	0 - 0.5T	ρ = 100Ω-M
	0.5T - T	ρ = 50Ω-M
MODEL 6	0 - T	ρ = 33Ω-M

5. Determination of Sea Ice Thickness with Airborne Electromagnetics

5.1 Survey Principles and Choice of System

At an early stage of this research project, it became evident that the problem of mapping ice thickness with airborne electromagnetics reduced to the problem of determining precisely the vertical distance from the sensor to the surface of the conductive sea water. Once this quantity is known then one simply subtracts from it the vertical distance from the sensor to the ice-air interface as determined by a precise radar or laser altimeter. The difference between these two quantities, i.e. distance between sensor and sea surface and distance between sensor and ice surface of course faithfully represents the ice thickness.

It is unfortunately impossible to accurately establish the sensor-conductor distance using a towed-bird system without knowing, at all times, the position of the bird that contains the receiver. Because this feature is not presently available on any towed-bird system, we have automatically rejected the use of a time domain system for the purpose of determining the sea ice in thickness from an aircraft. Consequently, all subsequent discussion is centered on the results that can be obtained with a rigid-boom frequency domain system.

5.2 Feasibility

In order to quickly assess the feasibility of using a helicopter towed, rigid-boom electromagnetic system for the determination of sea ice thickness, we computed the system response for a device with a co-axial receiver and a transmitter separated by a distance of six meters. The results are presented in Figure 7 in the form of an Argand diagram. The axes are conventionally labeled in parts per million of the primary field at the receiver. The plot is also characterized by two sets of parameters namely the vertical distance between the instrumentation boom and the surface of the conductor and "FC", the frequency-conductivity product for the conductor. In these calculations it was assumed that the sea ice if any was infinitely resistive. As presented, the data is valid for any 6m system. For example if we use a hypothetical 6m - 1000 hz system and obtain a reading of -90ppm quadrature and -280ppm in phase (this reading is located at point "A" on the chart shown in Figure 7) then we can deduce that the sea water conductivity is 4 S/m and that the system is at about 31.25m above the surface of the water. If in addition to this we had an altimeter reading to show a distance of 30m to the ice surface then an ice thickness of 1.25m can be inferred immediately.

The heavy dashed line on the diagram indicates the data locus for the coaxial Aerodat system operating at a fre-

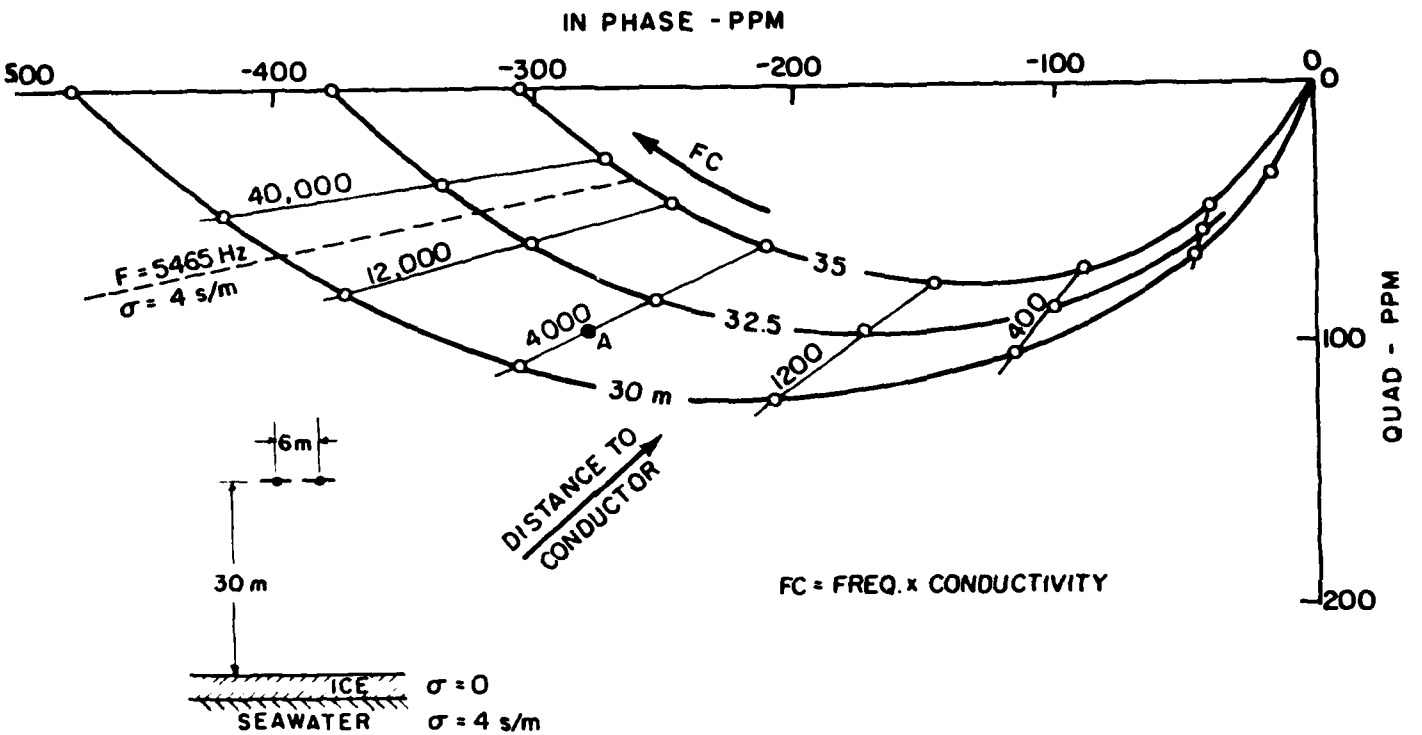

FIGURE 7 HELICOPTER SYSTEM RESPONSE

quency of 5465 hz. A value of 4 S/m is assumed for the sea water conductivity. At this point it is worthwhile to note that the ratio of the quadrature to the in phase response is fairly constant. Thus the phase of the secondary field varies only slightly with distance to the sea water surface, the amplitude of the response however, is very strongly dependent on this quantity.

The amplitude of the secondary field for the Aerodat system at 5465 hz above 4 S/m sea water is plotted as a function of height and/or ice thickness in Figure 8. We note a gradient of about 30 ppm/m of ice thickness. Allowing for a system noise of 1 ppm one can immediately conclude that under ideal conditions, this system could detect ice thickness variations of as little as 3 cm!

In order to estimate the magnitude of error that might be encountered in using the graph shown in Figure 8, which was computed under the assumption of infinitely resistive ice, to interpret data that is related to ice of finite conductivity we have computed theoretical data for ice models 1 and 6. Model 6 represented young ice with an average resistivity of 33 Ohm-m, Model 1 represented multi-year ice with a gradational resistivity profile. The theoretical data for these models were then "interpreted" using the graph of Figure 8. The results of this operation are tabulated in Table 3 and clearly indicate that finite ice resistivity is a very minimal source of error. To all intents and purposes sea

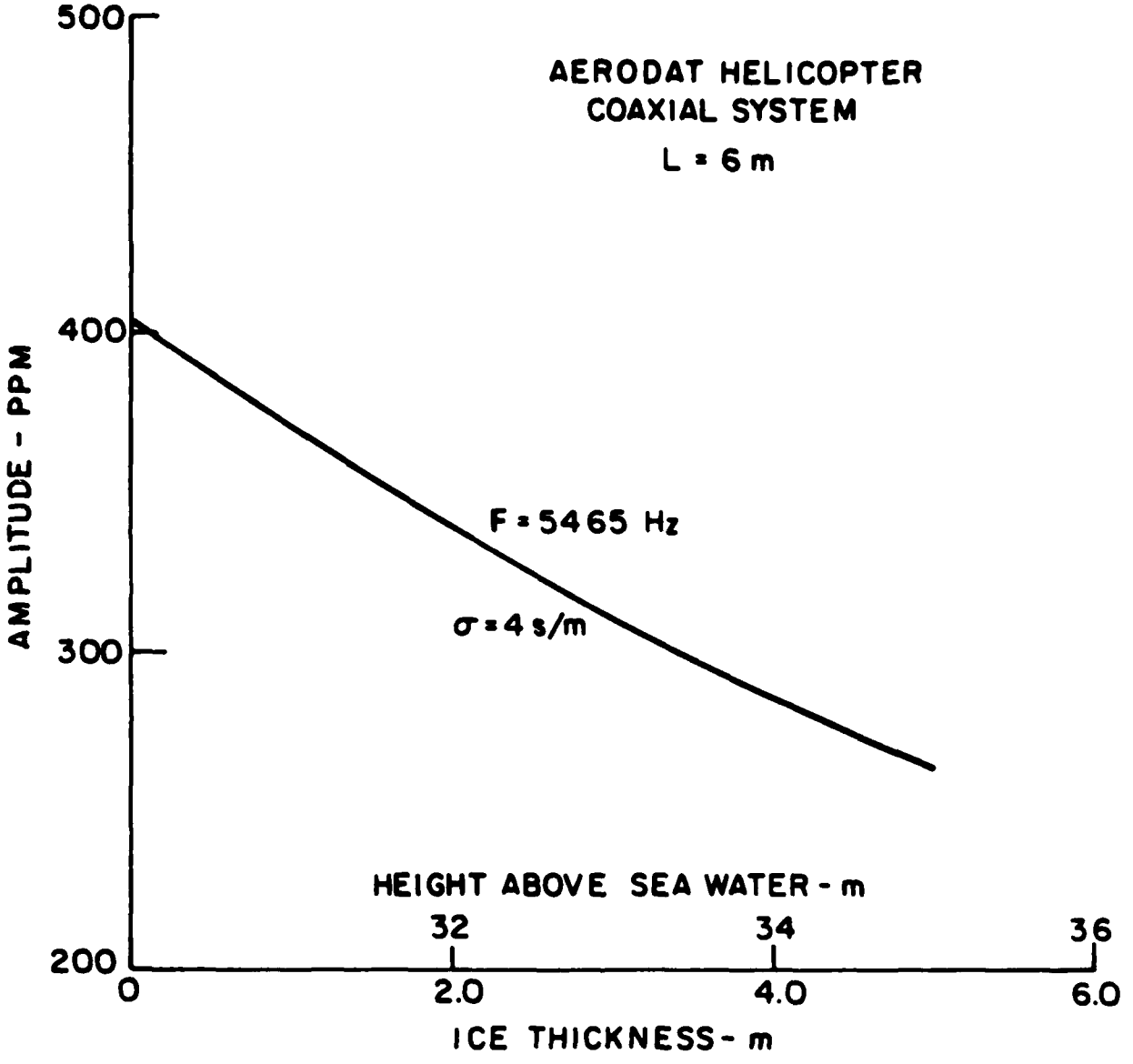

FIGURE 8 SYSTEM RESPONSE

TABLE 3

ERRORS IN ICE THICKNESS ESTIMATES
RELATED TO FINITE CONDUCTIVITY OF ICE
AERODAT COAXIAL SYSTEM F= 5465 Hz

ICE THICKNESS M	FIRST YEAR ICE AVERAGE MODEL ρ = 33 Ω-M ERROR IN ESTIMATE CM	MULTI YEAR ICE GRADATIONAL MODEL 1 ERROR IN ESTIMATE CM
1.00	--	--
2.00	-3	-3
3.00	-3	-3
4.00	-8	-8
5.00	-8	-8

ice is transparent to audio frequency electromagnetic energy.

It is more costly, from the view point of accuracy, to ignore the effects of the sea water conductivity and its depth. The simple method of data interpretation that relies on the ideal data shown in Figure 8 will at worst result in a 15% error in the estimated ice thickness for a 50% variation in sea water conductivity. Thus if the sea water conductivity is 3 S/m, instead of the supposed 4 S/m, a 2 m layer of ice will appear to be only 175cm thick. The effects of changes in sea water conductivity however can be accounted for by using a more complicated system of data interpretation based on charts such as that shown in Figure 7 which allows for estimates of both sea ice thickness and water conductivity.

Neglecting the fact that the sea ice can be floating on an inadequately thick layer of water can also cause very great errors in the estimates of ice thickness. In fact, good ice thickness estimates can only be obtained where the sea water is at least one skin depth (or about 3.5 m at 5465 Hz) deep. In areas where the water is shallower the effects of bottom conductivity would be difficult to separate out using only a single frequency measurement.

We have also examined the possibility of using the fixed wing Kenting/Scintrex Tridem system that operates at 8000 hz and normally flies at about 50m above the surface.

In a manner analogous to Figure 8, the amplitude response for this system is shown in Figure 9. Here we note a gradient of about 250 ppm/m of sea ice. The system noise however is about 25 ppm and thus its resolution is only about ± 10 cm under the best of circumstances.

5.3 An Optimal AEM System for Mapping the Thickness of Sea Ice

The definition of an optimal airborne electromagnetic system for mapping the thickness of sea ice can best be done in terms of a number of specific criteria. We must have a system that is;

(1) Simple to install

(2) Simple to operate

(3) Yields data that can be interpreted in real time.

(4) Demonstrates adequate (± 10 cm) sensitivity to ice thickness variations.

(5) Is relatively insensitive to variations in other parameters such as:

   a. ice resistivity
   b. water resistivity
   c. water depth

(6) Can be installed on a fixed wing aircraft to allow for missions of long duration.

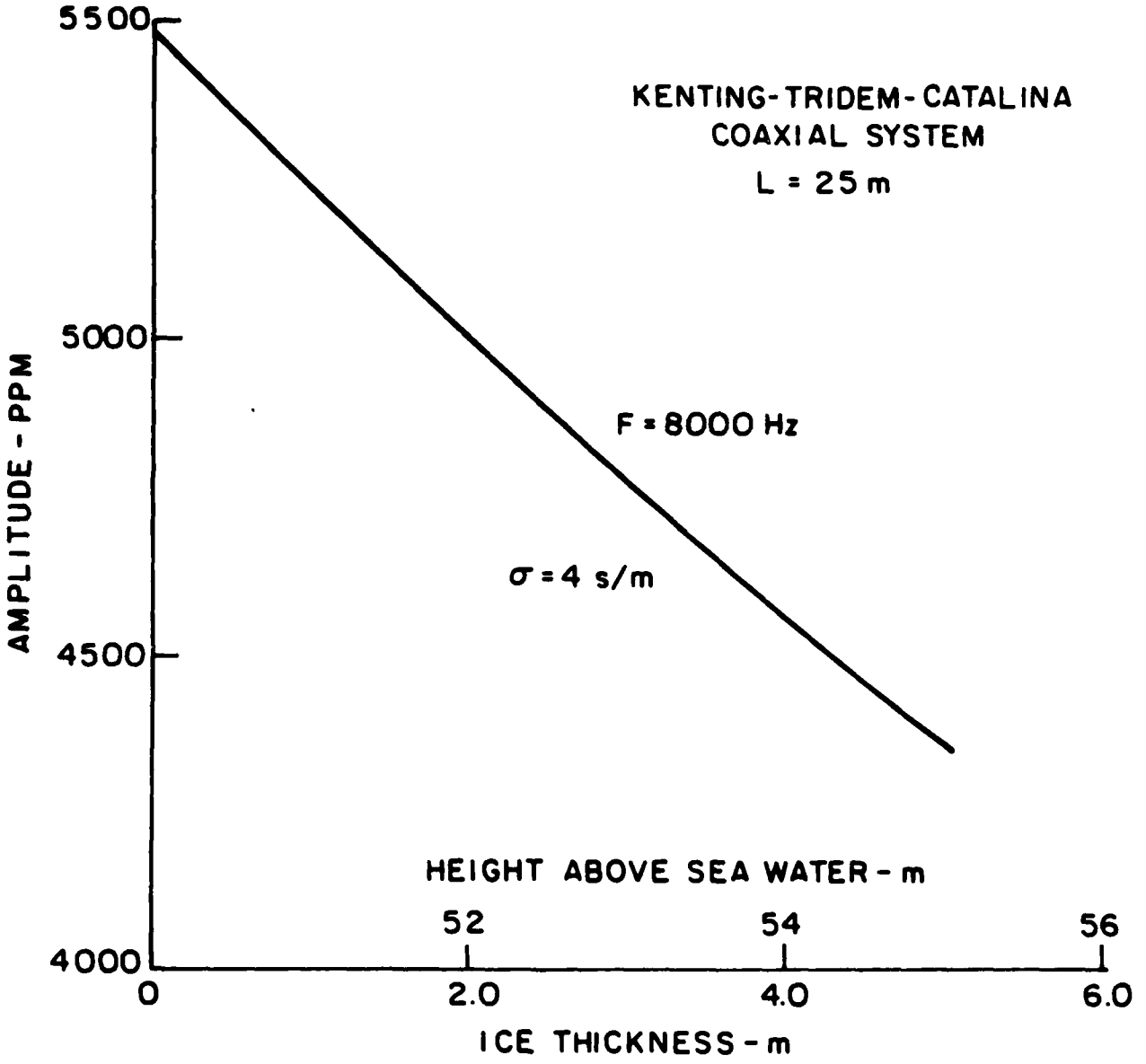

FIGURE 9 SYSTEM RESPONSE

A system that respons to all these criteria could be installed on a slow flying modern amphibian aircraft such as the Canadair CL 144. In order to take advantage of existing technology we suggest a horizontal axis transmitter. Simplicity of operation and good sensitivity to ice thickness will be obtained with a vertical axis receiver mounted in a tail stinger. A reasonable transmitter-receiver separation for this type of system would be 20 m. It could be flown at 50 m above the ice surface.

The frequency of operation must be chosen in a way that renders the system very sensitive to the position of the sea water-ice interface but not to the electrical properties of either the sea ice or the sea water. In particular one would like to use a frequency for which both young or multi-year sea ice will be transparent while at the same frequency, even moderately saline sea water would constitute a perfect reflector. After some detailed inspection of these criteria 30,000 Hz appears to be a frequency that satisfies these requirements.

Under these assumptions, we can readily use electromagnetic image theory (Keller and Frischknecht 1966, pp. 327-328) to predict the system response. This theory assigns an "infinite" conductivity to the conducting medium so that the conductor insulator interface (sea water-sea ice in our case) forms a perfect reflector for the source. In spite of this approximation this theory can give useful results in a

number of situations (Duckworth, 1974).

In our case, as will be demonstrated by comparing the exact numerical data and approximate results obtained from image theory, this theory can be used to quite accurately predict the optimal system response if the computation is done as follows:

Let P = the 30 Khz in phase component of the secondary field.

Let Q = the associated quadrature component

Let $A = P + Q$ (1)

denote the "image" anomaly.

Then, as suggested by the relations given by Keller and Frischknecht (1966, p. 340), "A" as defined above constitutes an excellent approximation to the ideal "image theory" system response.

For the optimal system in question, the guiding relations are:

$h = a + t$ (2)

h = system distance to water surface

a = system altitude above ice

t = ice thickness.

If "l" denotes the system coil separation then the system response is given by:

$$A = 3[l/h]^4 / [4+l^2/h^2]^{5/2} \quad (3)$$

The geometrical quantities used in this expression are shown in Figure 10. Figure 11 shows the system response as a function of ice thickness. Allowing for the fact that the ice thickness is much smaller than the system altitude and that the coil separation is also small in comparison with the system's distance to the water surface it is possible to immediately derive a simple approximate relationship for the system response. This turns out to be:

$$A = [3/32][1/a]^4 [1-4t/50] \qquad (4)$$

For the suggested optimal system (20m coil separation, 50m altitude) equation 4 simplifies further to;

$$A \simeq 2400[1-4t/50] \text{ ppm} \qquad (5)$$

This expression is only accurate to about 10% when compared with the corresponding values obtained from equation 3. It does however correctly indicate a gradient of about 200 ppm per meter of sea ice. Thus if we are to resolve about 5 cm of ice the optimal system need only have a noise level of 10ppm.

We next examine the effects of sea ice conductivity on the correct estimate of its thickness using image theory. This is done in Table 4 which illustrates this problem for a 2 meter thick slab. The accuracy of the image method is

TABLE 4

Influence of Sea Ice Resistivity on Optimal System Response
L=20M, A=50M, F=30kHz
Nominal Ice Thickness - 2.0M

Ice Resistivity Ω-m (see Table 2)	Real ppm P	Quad ppm Q	Corrected Real ppm A = P + Q	Estimated Thickness m
∞	1775	94	1869	2.02
33	1795	99	1894	1.86
100	1764	95	1859	2.59
Model 2	1792	100	1892	1.88
Model 3	1781	98	1879	1.96
Model 4	1778	96	1874	2.00
Model 5	1777	96	1873	2.00

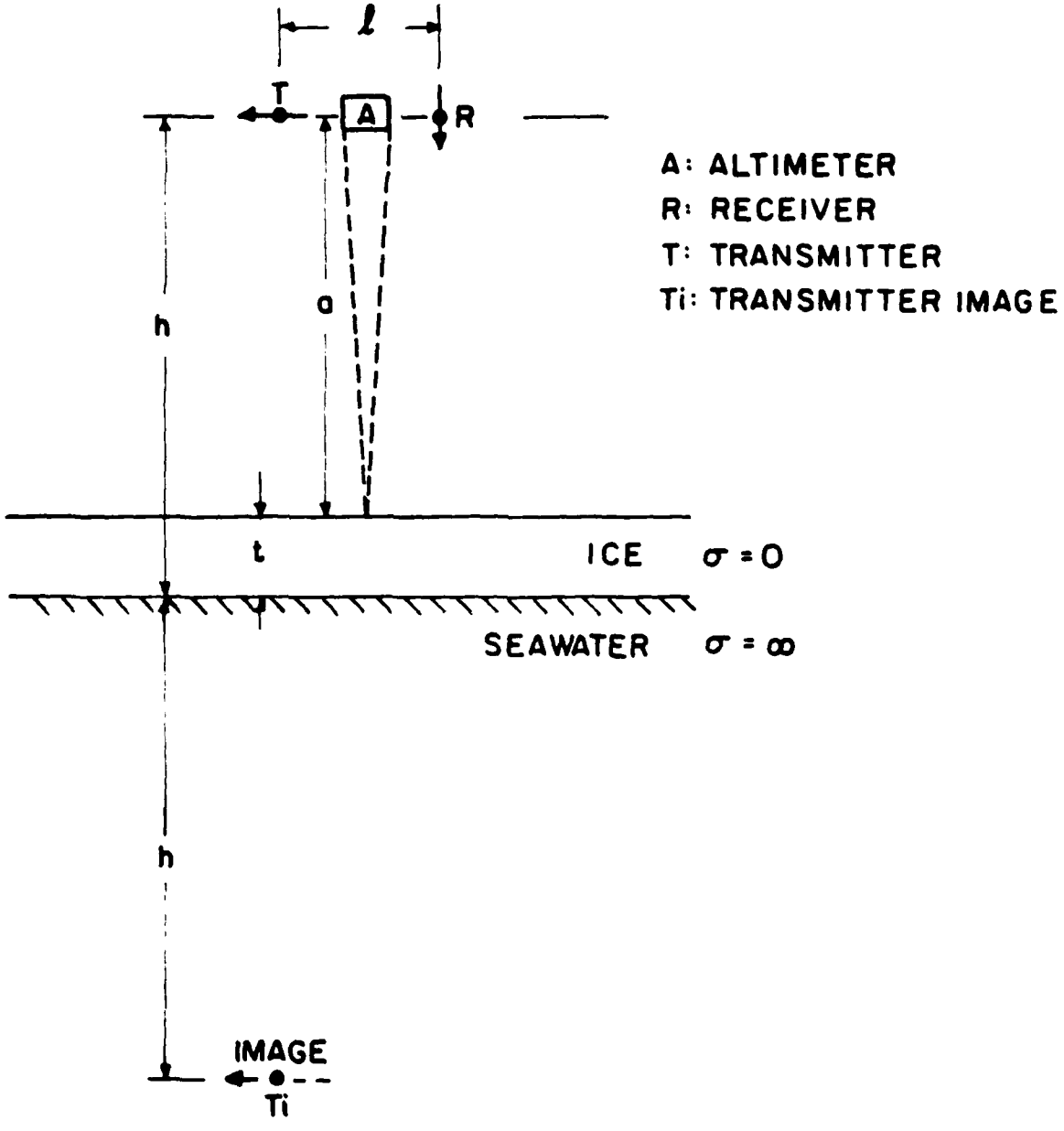

FIGURE 10 IMAGE THEORY PARAMETERS

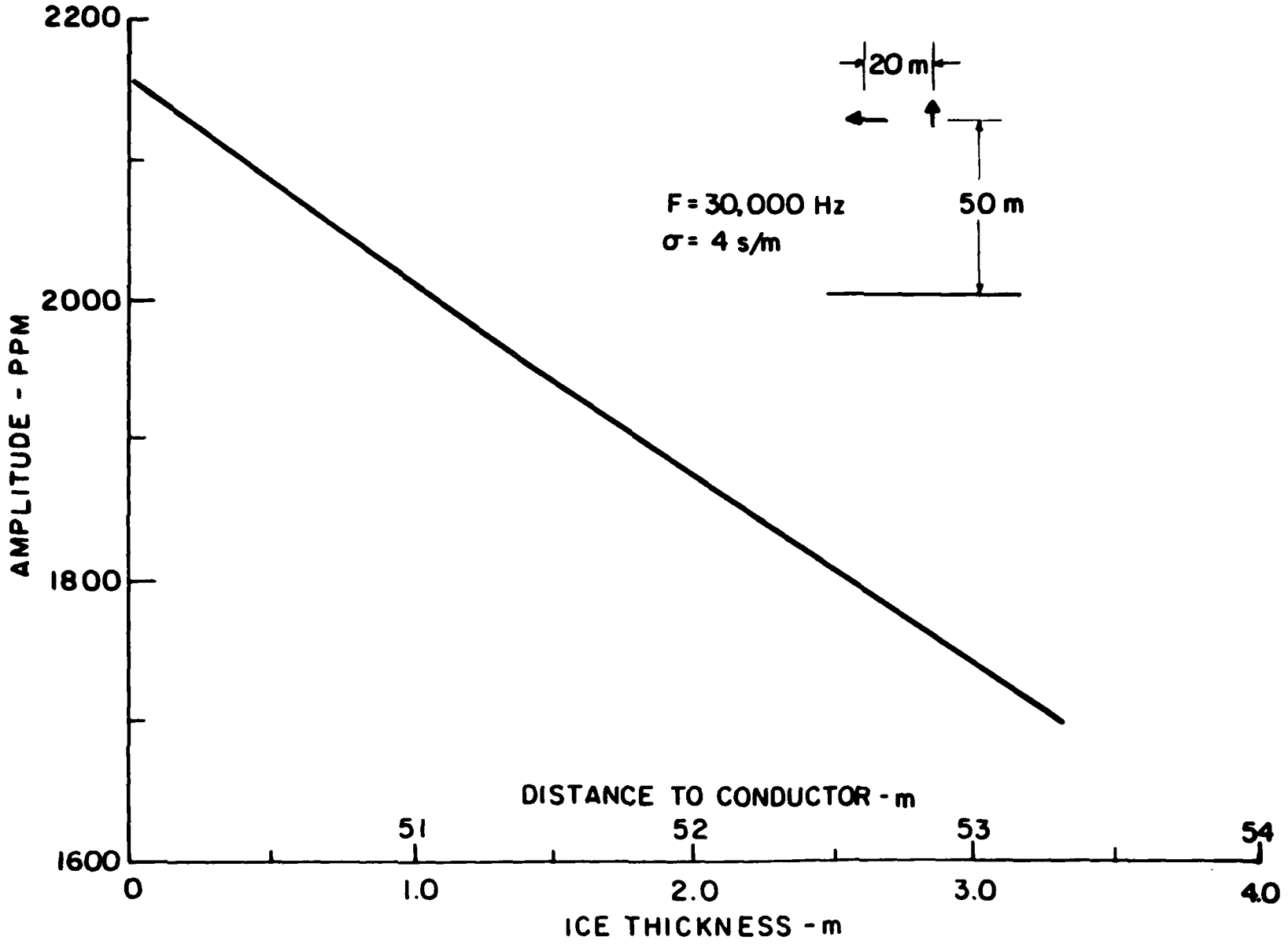

FIGURE 11 OPTIMAL SYSTEM RESPONSE

surprisingly good showing the worst case error of 14 cm for young ice.

The effects of sea water conductivity on ice thickness estimates as seen for a 2 meter layer of 33 ohm-m ice are examined in Table 5. Again, the proper use of image theory renders this effect minimal with the worst error amounting to but 14 cm or 7%. The effects of sea water depth on ice thickness estimates were not examined for the optimal system. It is believed however, that as previously mentioned the water must be at least one skin depth deep in order to correctly estimate ice thickness. At the high operating frequency of the optimal system this requirement is trivial as it amounts to 1.5m of sea water.

6. Conclusions and Recommendations

On the basis of the foregoing discussion one can readily conclude that it is quite feasible to measure the thickness of sea ice in the polar regions using an airborne electromagnetic system. In order to avoid the errors related to receiver motion the measurements must be made in the frequency domain usng a rigidly coupled apparatus. In principle either a helicopter towed boom equipment or a fixed wing apparatus can be used for the purpose. The former is preferred for small scale surveys because of its "button-on" adaptability to any number of carrier vehicles. For long range large scale surveys the fixed wing version is preferable.

TABLE 5

INFLUENCE OF SEAWATER CONDUCTIVITY
ON OPTIMAL SYSTEM RESPONSE
NOMINAL ICE THICKNESS 2. M
ICE RESISTIVITY 33Ω-M
F = 30,000 Hz

SEAWATER CONDUCTIVITY S/M	REAL PPM	QUAD PPM	CORRECTED REAL PPM	ESTIMATED THICKNESS M
4	1795	99	1894	1.86
3	1765	112	1877	1.98
2	1741	135	1876	1.98
1	1687	183	1870	2.02

There is no doubt that conventional survey equipment available now for contract work would give valuable results. It can be used to verify the theoretical ideas presented here and to assure us that no possible sources of error have been ignored. There is little to choose between the various commercial systems listed in Table 1.

Finally, we conclude that the simple electromagnetic image theory can be used to predict the response of an optimal system for mapping the thickness of sea ice. A system that uses this technique for data interpretation can readily translate the observed secondary field amplitudes in terms of an underlying ice thickness.

Because the determination of sea ice thickness with an airborne electromagnetic device is entirely feasible we strongly recommend that the concepts outlined in this report be subjected to a comprehensive field test. This test sould be carried under operating conditions similar to those envisaged for future practical application of this technique. We suggest the use of a helicopter towed system that will be equipped with a precise altimeter located on the same boom as the electromagnetic sensors. Ground verification of the airborne thickness determinations can be done by a number of drilled holes. Advantage should be taken of the drilling program to carry out a limited amount of measurements on the electrical properties of sea ice.

REFERENCES

Barringer, A. R. 1962, The INPUT electrical pulse prospecting system; Min. Cong. J., vol. 48, pp. 49-52.

Becker, A. 1969, Simulation of time-domain, airborne, electromagnetic system response, Geophysics, vol. 34, pp. 739-752.

Becker, A. 1979, Airborne electromagnetic methods, Geophysics and Geochemistry in the Search for Metallic Ores; Peter J. Hood, editor; Geological Survey of Canada, Economic Geology Report 31, pp. 33-43.

DeMoully, G.T. and Becker, A., 1982, Automated interpretation of airborne electromagnetic data. Abstract. Technical Program, 52nd Annual Mtg. S.E.G. pp. 382-384.

Duckworth, K. 1970, Electromagnetic depth sounding applied to mining problems. Geop. vol. 35, pp. 1086-1098.

Fraser, D.C. 1979, The multicoil II airborne electromagnetic system, Geophysics, vol. 44, pp. 1367-1394.

Keller, G.V. and Frischknecht, F.C., 1966, /Electrical methods in geophysical prospecting, Pergamon Press, N.Y.

McNeill, D. and Hoekstra, P., 1975, In situ measurements on the conductivity and surface impedance of sea ice at VLF. Radio Science, vol. 8, #1, pp. 23-30.

Morrison, H.F. and Becker, A., 1982, Analysis of airborne electromagnetic systems for mapping depth of sea water. Final report, ONR contract #N 00014-82-M-0073, 57p. U.C.B.-Engineering Geoscience

Pitcher, D.H., Barlow, R.B., and Lewis, M., 1980, Tridem airborne conductivity mapping as a lignite exploration method, CIM Bulletin, May, pp. 1-12.

Sinha, A.K. (1976), A field study for sea ice thickness determination by electromagnetic means. Geol. Surv. Can. Paper 76-1C, pp. 225-228.

Distribution List

Department of the Navy
Asst Deputy Chief of Navy Materials
for Laboratory Management
Rm 1062 Crystal Plaza Bldg 5
Washington DC 20360

Department of the Navy
Asst Secretary of the Navy
(Research Engineering & System)
Washington DC 20350

Project Manager
ASW Systems Project (PM-4)
Department of the Navy
Washington DC 20360

Department of the Navy
Chief of Naval Material
Washington DC 20360

Department of the Navy
Chief of Naval Operations
ATTN: OP 951
Washington DC 20350

Department of the Navy
Chief of Naval Operations
ATTN: OP 952
Washington DC 20350

Department of the Navy
Chief of Naval Operations
ATTN: OP 987
Washington DC 20350

Director
Chief of Naval Research
ONR Code 420
ATTN: Dr. G. B. Morris
Ocean Science & Technology Det
NSTL, MS 39529

Director
Defense Technical Info Cen
Cameron Station
Alexandria VA 22314

Commander
DW Taylor Naval Ship R&D Cen
Bethesda MD 20084

Commanding Officer
Fleet Numerical Ocean Cen
Monterey CA 93940

Director
Korean Ocean R&D Inst
ATTN: K. S. Song, Librarian
P. O. Box 17 Yang Jae
Seoul South Korea

Commander
Naval Air Development Center
ATTN: Dr. A. R. Ochadlick, Jr.
Warminster PA 18974

Commander
Naval Air Systems Command
Headquarters
ATTN: Code 340J (Mr. Barry Dillon)
Code 330G (Dr. Paul F.
Twitchell)
Washington DC 20361

Commanding Officer
Naval Coastal Systems Center
Panama City FL 32407
ATTN: Code 4130 (Dr. G. Kekelis)

Commander
Naval Electronic Sys Com
Headquarters
Washington DC 20360

Commanding Officer
Naval Environmental Prediction
Research Facility
Monterey CA 93940

Commander
Naval Facilities Eng Command
Headquarters
200 Stovall St.
Alexandria VA 22332

Commanding Officer
Naval Ocean R & D Activity
ATTN: Codes 110/111
Code 125
Code 200
Code 300
Code 115
Code 500
NSTL MS 39529

Director
Liaison Office
Naval Ocean R & D Activity
800 N. Quincy Street
502 Ballston Tower #1
Arlington VA 22217

Commander
Naval Ocean Systems Center
San Diego CA 92152

Commanding Officer
Naval Oceanographic Office
ATTN: Code 8000
Code 8200
Code 8400
Code 8402
NSTL MS 39522

Commander
Naval Oceanography Command
ATTN: Larry Reshew
NSTL MS 39522

Superintendent
Naval Postgraduate School
ATTN: Dr. O. Heinz, Code 61 Hz
Monterey CA 93940

Commanding Officer
Naval Research Laboratory
Washington DC 20375

Commander
Naval Sea System Command
Headquarters
ATTN: Daniel Porter, Code 63 R1
Washington DC 20362

Commander
Naval Surface Weapons Center
Dahlgren VA 22448

Commanding Officer
Naval Underwater Systems Center
ATTN: New London Lab
Newport RI 02840

Director
New Zealand Oceano Inst
ATTN: Library
P. O. Box 12-346
WELLINGTON N., NEW ZEALAND

Director
Office of Naval Research
Ocean Science & Technology Div
NSTL MS 39529

Department of the Navy
Office of Naval Research
ATTN: Code 102
800 N. Quincy St.
Arlington VA 22217

Commanding Officer
ONR Branch Office
536 S Clark Street
Chicago IL 60605

Commanding Officer
ONR Branch Office LONDON
Box 39
FPO New York 09510

Commanding Officer
ONR Western Regional Ofs
1030 E. Green Street
Pasadena CA 91106

President
Texas A&M
ATTN: Dept of Ocean Working Collection
College Station TX 77843

Director
University of California
Scripps Institute of Oceanography
P. O. Box 6049
San Diego Ca 92106

Director
Woods Hole Oceanographic Inst
Woods Hole MA 02543

Chief of Naval Material
(MAT-0724)
ATTN: Capt. John Harlett
800 N. Quincy St.
Arlington, VA 22217

EUREKA Resources Associates, Inc.
ATTN: R. O. Prindle
2161 Shattuck Avenue, Suite 317
Berkely, CA 94704

SRI International
Electromagnetics Science Laboratory
ATTN: A. M. Buberie
333 Ravenswood Avenue
Menlo Park, CA 94025

Rockwell International
Missile System Division
ATTN: S. Stasenko
3370 Miraloma Avenue
Anaheim, CA 92803

Geological Survey of Canada
Terrain Geophysics Subdivision
ATTN: L. S. Collett
601 Booth St.
Ottawa, Ontario
Canada K1A0E8

Dobrocky Seatech Limited
ATTN: Dr. J. R. Harper
9865 West Suanich Rd.
P. O. Box 6500
Sidney, British Colombia

Geophex, Ltd.
ATTN: Dr. I. J. Won
319 Morrison Avenue
Raleigh, NC 27608

International Exploration, Inc.
ATTN: T. L. Jacobsen
577 Sackettsford Road
Warminster, PA 18974-1398

Carson Geoscience Company
ATTN: A. J. Navazio
32-H Blooming Glen Road
Perkasic, PA 18944

Airborne Systems, Inc.
ATTN: R. L. Summerfelt
10700 Walker St.
Cypress, CA 90630

Westinghouse Electric Corporation
Defense Group
ATTN: H. L. Hamrick
98 Miracle Strip Parkway
Ft. Walton Beach, FL 32548

EG&G Washington Analytical Service
Center, Inc.
Attn: G. L. Bill
2150 Fields Rd.
Rockville, MD 20850

Geotech, Ltd.
ATTN: E. B. Morrison
21-101 Amber Street
Markham, Ontario
Canada L3R 3B2

Barringer Research Ltd.
ATTN: C. Cumming
304 Carlingview Drive
Rexdale, Ontario
Canada M9W 5G2

Dynamics Technology, Inc.
ATTN: S. R. Borchandt
22939 Hawthorne Blvd.
Torrance, CA 90505

Chief of Naval Research
ONR
ATTN: Dr. C. A. Luther, Code 425AR
Dr. T. Warfield, Code 220
Washington, DC 20350

UNCLASSIFIED

SECURITY CLASSIFICATION OF THIS PAGE (When Data Entered)

REPORT DOCUMENTATION PAGE		READ INSTRUCTIONS BEFORE COMPLETING FORM
1. REPORT NUMBER NORDA Technical Note 261	2. GOVT ACCESSION NO. AD-A139 786	3. RECIPIENT'S CATALOG NUMBER
4. TITLE (and Subtitle) ANALYSIS OF AIRBORNE ELECTROMAGNETIC SYSTEMS FOR MAPPING THICKNESS OF SEA ICE		5. TYPE OF REPORT & PERIOD COVERED Final
		6. PERFORMING ORG. REPORT NUMBER
7. AUTHOR(s) A. Becker H. Morrison K. Smits		8. CONTRACT OR GRANT NUMBER(s)
9. PERFORMING ORGANIZATION NAME AND ADDRESS Naval Ocean Research and Development Activity Ocean Science Directorate NSTL, Mississippi 39529		10. PROGRAM ELEMENT, PROJECT, TASK AREA & WORK UNIT NUMBERS 62759N
11. CONTROLLING OFFICE NAME AND ADDRESS Same		12. REPORT DATE November 1983
		13. NUMBER OF PAGES 38
14. MONITORING AGENCY NAME & ADDRESS(if different from Controlling Office)		15. SECURITY CLASS. (of this report) UNCLASSIFIED
		15a. DECLASSIFICATION DOWNGRADING SCHEDULE

16. DISTRIBUTION STATEMENT (of this Report)

Approved for Public Release
Distribution Unlimited

17. DISTRIBUTION STATEMENT (of the abstract entered in Block 20, if different from Report)

18. SUPPLEMENTARY NOTES

19. KEY WORDS (Continue on reverse side if necessary and identify by block number)

ice thickness
airborne electromagnetic (AEM)
airborne mapping
geophysical prospecting

20. ABSTRACT (Continue on reverse side if necessary and identify by block number)

NORDA Code 372 is at present engaged in research projects for extending Airborne Electromagnetic (AEM) technology from geophysical prospecting applications to Navy requirements such as airborne shallow water bathymetry, airborne ice thickness determination, and conductivity profiling. This report is part of our research program addressing AEM ice thickness determination and will demonstrate that the Navy requirements for rapid airborne methods for mapping ice thickness, in real time, can be accomplished with Aem techniques. At present

DD FORM 1 JAN 73 1473 EDITION OF 1 NOV 65 IS OBSOLETE
S/N 0102-LF-014-6601

UNCLASSIFIED
SECURITY CLASSIFICATION OF THIS PAGE (When Data Entered)

there are no reliable airborne techniques for measuring sea ice, although impulse radar has yielded promising results over fresh-water ice but not over sea-water ice.

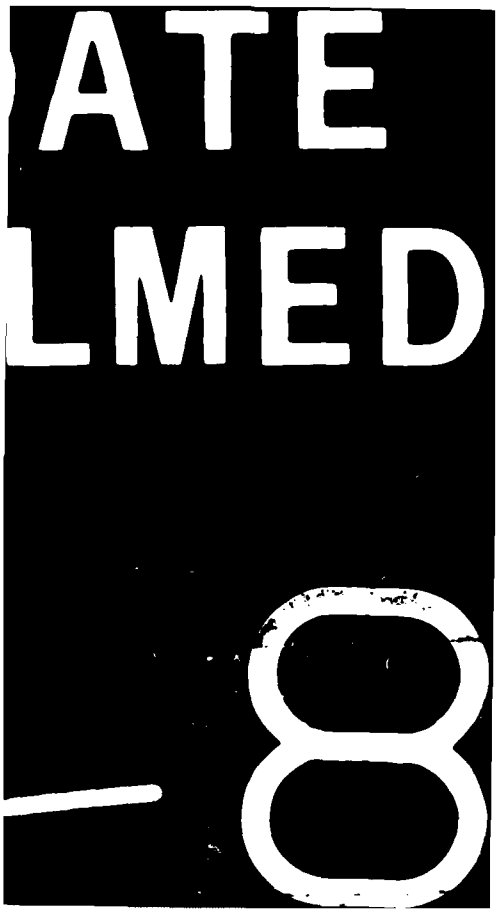
ATE
LMED
8